EDGE ARTICLE

Check for updates

Ionic organic cage-encapsulating phase-transferable metal clusters†

Su-Yun Zhang, [ID] [a] Zdravko Kochovski, [c] Hui-Chun Lee, [a] Yan Lu, [ID] [cd] Hemin Zhang, [e] Jie Zhang, [ID] [a] Jian-Ke Sun*[a] and Jiayin Yuan [ID] *[b]

Exploration of metal clusters (MCs) adaptive to both aqueous and oil phases without disturbing their size is promising for a broad scope of applications. The state-of-the-art approach *via* ligand-binding may perturb MCs' size due to varied metal–ligand binding strength when shuttling between solvents of different polarity. Herein, we applied physical confinement of a series of small noble MCs (<1 nm) inside ionic organic cages (I-Cages), which by means of anion exchange enables reversible transfer of MCs between aqueous and hydrophobic solutions without varying their ultrasmall size. Moreover, the MCs@I-Cage hybrid serves as a recyclable, reaction-switchable catalyst featuring high activity in liquid-phase NH_3BH_3 (AB) hydrolysis reaction with a turnover frequency (TOF) of 115 min^{-1}.

Introduction

Metal clusters (MCs) are particles of <2 nm in size and exhibit intrinsic size-dependent properties, such as discrete electronic structures, intense photoluminescence, high catalytic activity (such as oxidation, hydrogenation, and coupling reactions), *etc.*[1] Synthesis of MCs capable of adapting both aqueous and organic phases is favorably pursued because of a broader scope of operational environment.[2] MCs, especially of size <1 nm practically carry all constitutional atoms on their surface, and possess a higher specific surface energy than the exhaustively explored larger metal nanoparticles (MNPs).[3] Thus they aggregate more severely without sufficient protection in solutions.[4,5] Synthetic methods of MCs are so far dominated by the surface-binding ligand approach, including amphiphilic capping agents, and the oil–water phase transfer agents by either ligand exchange or modification.[2,6] A challenge associated with the ligand approaches that relies on binding active sites of MCs is that the MC core is labile and prone to size variation due to altered metal–ligand

binding strength upon ligand exchange or modification.[7] In addition, these approaches suffer from a trade-off, *i.e.* binding a high-energy, catalytically active surface by polar groups of ligands restricts accessibility of reactants to these active sites during catalysis.[8] In this regard, a stabilization mechanism of MCs majorly by physical confinement and partially by surface binding would allow MCs to maintain their high catalytic activity in different solvents with little-to-no perturbation of stabilization, thus possibly breaking the trade-off.

Organic molecular cages are an emerging class of multi-functional materials featuring a discrete pore structure.[9] They are molecularly soluble and possess a wide spectrum of properties and functions due to their designable molecular architecture and intrinsic open channels. A unique merit of cages is to accommodate guest objects, such as MCs/MNPs without blocking much of their active surface sites and to "solubilize" them in liquid-phase for catalysis.[10]

Herein, we utilized ionic organic cages to synthesize and confine a series of well-dispersed, water–oil phase adaptive noble MCs of 0.5–0.7 nm in size (Scheme 1). Different from MCs reported previously that have limited choices of metal species and/or solvents, our example improves compatibility between the ionic cage molecule and metal species. More significantly, the highly charged cage (+12 per cage) can trap metal anion precursor to control MC growth and avoid spontaneously aggregation by electrostatic repulsion. The MCs confined in I-Cage experience anion-controlled reversible water–oil phase transfer without size perturbation. Such MC@I-Cage hybrid was explored as recyclable/switchable catalyst[11] with high activity in a liquid-phase H_2 release reaction.

[a] MOE Key Laboratory of Cluster Science, Beijing Key Laboratory of Photoelectronic/Electrophotonic Conversion Materials, School of Chemistry and Chemical Engineering, Beijing Institute of Technology, Beijing, P. R. China. E-mail: jiankesun15@gmail.com

[b] Department of Materials and Environmental Chemistry, Stockholm University, 10691 Stockholm, Sweden. E-mail: jiayin.yuan@mmk.su.se

[c] Soft Matter and Functional Materials, Helmholtz-Zentrum Berlin für Materialien und Energie, 14109 Berlin, Germany

[d] Institute of Chemistry, University of Potsdam, 14467 Potsdam, Germany

[e] School of Energy and Chemical Engineering, Ulsan National Institute of Science & Technology (UNIST), Ulsan 689-798, Republic of Korea

† Electronic supplementary information (ESI) available: Experimental procedures, related characterizations and catalytic applications. See DOI: 10.1039/c8sc04375b
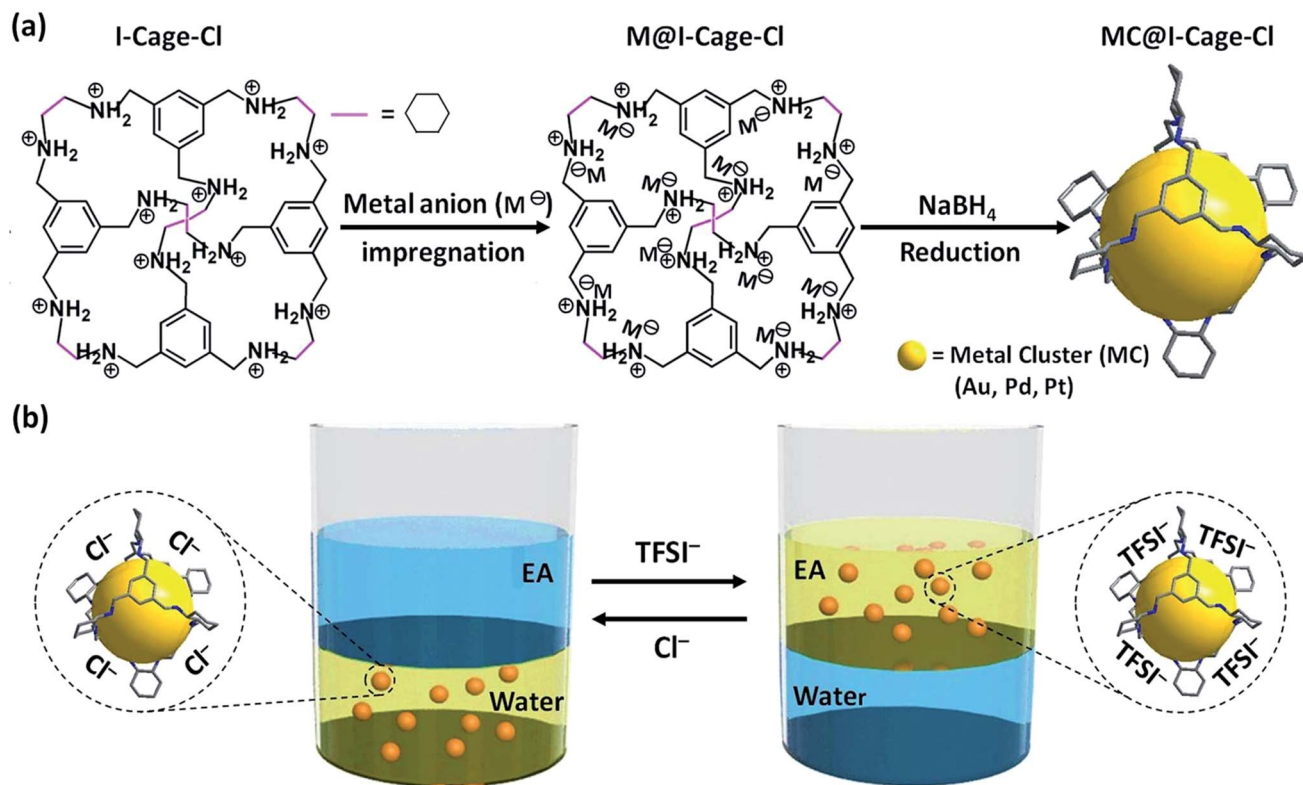
Scheme 1 (a) Synthetic scheme of MCs stabilized by I-Cage−Cl (Cl as counterion) in an aqueous phase (for clarity reasons Cl⁻ anions are omitted; $M^- = [AuCl_4]^-$, $[PdCl_4]^{2-}$ and $[PtCl_4]^{2-}$). (b) Anion exchange-driven phase transfer of I-Cage−X (X = Cl^- or $TFSI^-$, TFSI = bis(tri-fluoromethane sulfonyl)imide)-capped MCs between aqueous and ethyl acetate (EA) phases.

Experimental

Materials and methods

All chemicals were obtained from commercial sources and used without further purification. Conventional transmission electron microscopy (TEM) was performed on a JEOL 2010FS transmission electron microscope operated at 120 kV. The scanning TEM (STEM) was performed on a Jeol JEM-2200FS transmission electron microscope operated at 200 kV and equipped with a high-angle annular dark-field (HAADF) STEM detector. The cryogenic electron microscopy (Cryo-EM) was performed on a JEOL JEM-2100 transmission electron microscope (JEOL GmbH, Eching, Germany). Cryo-EM specimens were prepared by applying a 4 μL drop of a dispersion sample to Lacey carbon-coated copper TEM grids (200 mesh, Science Services) and plunge-frozen into liquid ethane with an FEI vitrobot Mark IV set at 4 °C and 95% humidity. Vitrified grids were either transferred directly to the microscope cryogenic transfer holder (Gatan 914, Gatan, Munich, Germany) or stored in liquid nitrogen. Imaging was carried out at temperatures around 90 K. The TEM was operated at an acceleration voltage of 200 kV, and a defocus of the objective lens of about 2.5–3 μm was used to increase the contrast. Cryo-EM micrographs were recorded at a number of magnifications with a bottom-mounted 4 × 4k CMOS camera (TemCam-F416, TVIPS, Gauting, Germany). The total electron dose in each micrograph was kept below 20 e⁻ Å⁻². X-ray photoelectron spectroscopy (XPS) studies were performed on a ThermoFisher ESCALAB250 X-ray photo-electron spectrometer (powered at 150 W) using Al Kα radiation ($\lambda = 8.357$ Å). To compensate surface charging effects, the XPS spectrum was referenced to the C 1s neutral carbon peak at 284.6 eV. The solution UV-Vis absorption measurements were recorded on a Lambda 900 spectrophotometer. ^{1}H and ^{13}C nuclear magnetic resonance (^{1}H-NMR and ^{13}C-NMR) measurements were carried out at room temperature on a Bruker ascend-400/600 spectrometer in D_2O and $CDCl_3$. Dynamic light scattering (DLS) was performed on a NICOMP particle sizer (model 380 PSS, Santa Barbara, CA). Zeta potential measurement was performed on Zetasizer Nano ZS90 (Malvern). Electrospray ionisation mass spectrometry (ESI-MS) was performed on 1200 Series & HCT Basic System (Bruker). Inductively coupled plasma optical emission spectrometry (ICP-OES) was performed on Varian 700-ES (Agilent), calibrated with standard solutions.

Synthesis of porous cycloimine cage molecule CC3

The synthesis of CC3 was conducted according to a previous method.[10a] A typical procedure is as follows: CH_2Cl_2 (10 mL) was added slowly to solid 1,3,5-triformylbenzene (0.5 g) at room temperature. Trifluoroacetic acid (10 μL) was added directly to this solution as a catalyst for imine bond formation. Finally, a CH_2Cl_2 solution (10 mL) of (R,R)-1,2-diaminocyclohexane (0.5 g, 4.464 mmol) was added. The vessel of the mixture

solution was capped and left to stand for one week. Crystals grew on the sides of the vessel. The crystalline product was removed by centrifugation and washed with CH_2Cl_2/CH_3OH mixture (v/v, 5/95) for several times, and further dried at 100 °C overnight. The ^1H NMR spectrum is consistent with reported CC3 (Fig. S36†).

Synthesis of reduced CC3 (RCC3)

The synthesis of RCC3 was conducted according to a previous method.[12a,c] The imine cage CC3 (463 mg) was dissolved in a CH_2Cl_2/CH_3OH mixture (v/v, 1/1, 25 mL) by stirring. When this solution became clear, $NaBH_4$ (0.5 g) was added and the reaction was stirred for 15 h at room temperature. Water (1 mL) was then added, and the solution was continuously stirred for additional 9 h. The solvent was then removed under vacuum. The resulted solid was washed by water and collected by centrifugation, and the obtained solid was dried at 80 °C under vacuum overnight. The ^1H NMR spectrum is consistent with reported RCC3 (Fig. S37†).

Synthesis of I-Cage–Cl[12b]

RCC3 (500 mg) was dissolved in $CHCl_3$ (10 mL) by stirring. Hydrogen chloride (in dioxane, 2.50 mL) was added dropwise. The precipitate appeared and the reaction mixture was stirred for a further 2 h at room temperature. The precipitate was collected by filtration then washed by $CHCl_3$ for several times to give solid powder after being dried under vacuum at 90 °C. ^1H NMR (D_2O, 400 MHz) δ 7.62 (s, 12H, –ArH), 4.47 (d, 12H, –ArCH₂), 4.23 (d, 12H, –ArCH₂), 3.69 (d, 12H, CH on cyclohexane), 2.55–1.27 (m, 48H, CH_2 on cyclohexane) ppm (the details of peak integration are shown in Fig. S38†); ^{13}C NMR (D_2O, 400 MHz): δ 133.0, 130.0, 58.5, 48.3, 25.8, 22.6 ppm. The reported RCC3 formula is $C_{72}H_{108}N_{12}$ ($M = 1141.73$),[12a] accordingly, the estimated molecular formula for cationic cage part is $C_{72}H_{120}N_{12}$ (the 12 –NH– units per cage are fully protonated by acid, $M = 1154$). This is consistent with the ESI(+)-MS analysis result $[M + H]^+$ of 1155.5 (Fig. S3†).

Synthesis of metal cluster (MC)/metal nanoparticles stabilized by different supports

Synthesis of Au@I-Cage–Cl. In a typical synthesis, 9 mL of water solution containing 15 mg of I-Cage–Cl was subsequently added to 0.5 mL of aqueous $HAuCl_4$ solution (0.5 mg Au in content). The resultant mixture solution was further homogenized after aging for a few minutes. Then, 0.5 mL of aqueous solution containing 2 mg of $NaBH_4$ was immediately added into the above solution with vigorous shaking, resulting in a well transparent dispersion of Au@I-Cage–Cl. The sample could be isolated by drying under N_2 flow and then washed by $CHCl_3$.

Synthesis of other MCs stabilized by I-Cage–Cl. The synthetic procedure used above to prepare Au@I-Cage–Cl was followed by using 0.5 mL of aqueous containing K_2PdCl_4, or K_2PtCl_4 (the metal in content is 0.5 mg) in place of $HAuCl_4$ (^1H NMR: Fig. S39 and S40†).

Synthesis of Au/RCC3. The synthetic procedure used above to prepare Au@I-Cage–Cl was followed by using 9 mL of water

solution containing RCC3 (15 mg) in place of I-Cage–Cl (^1H NMR: Fig. S41†). The sample could be isolated by centrifugation and then washed by water.

Synthesis of Au/4-cyanomethyl-1-vinyl-imidazolium bromide. The synthetic procedure used above to prepare Au@I-Cage–Cl was followed by using 9 mL of water solution containing 4-cyanomethyl-1-vinyl-imidazolium bromide (15 mg) in place of I-Cage–Cl.

Phase transfer of Au@I-Cage–X (X = Cl⁻ or TFSI⁻) driven by anion exchange

Typically, 1 mL of as-synthesized Au@I-Cage–Cl (above section) was layered with 1 mL ethyl acetate (EA), then 3 mg LiTFSI was added into the solution and rigorously shaking to let Au@I-Cage–Cl transfer to EA (Au@I-Cage–TFSI) (the addition of a few drop of methanol (~50 μL) that is miscible in both water and EA can accelerate the transfer process). Then 6 mg KCl was added into the solution to achieve the reversible transfer to water solution.

Synthesis of catalyst for AB hydrolysis reaction

Synthesis of Pt@I-Cage–Cl catalyst. The synthetic procedure used above to prepare Au@I-Cage–Cl was followed by using 6 mL of aqueous solution containing I-Cage–Cl (15 mg), 0.5 mL of aqueous solution containing K_2PtCl_4, (0.01 mmol Pt in content) in place of $HAuCl_4$.

Synthesis of Pt/RCC3 catalyst. The synthetic procedure used above to prepare Pt@I-Cage–Cl catalyst was followed by using 6 mL of aqueous solution containing RCC3 (15 mg) in place of I-Cage–Cl.

Synthesis of Pt-support-free (Pt-SP-Free) catalyst. The synthetic procedure used above to prepare Pt@I-Cage–Cl catalyst was followed by using 6 mL of aqueous solution without I-Cage–Cl stabilizer.

Synthesis of Pt/CTAB catalyst. The synthetic procedure used above to prepare Pt@I-Cage–Cl catalyst was followed by using 6 mL of aqueous solution containing CTAB (15 mg) in place of I-Cage–Cl.

Synthesis of Pt/PVP catalyst. The synthetic procedure used above to prepare Pt@I-Cage–Cl catalyst was followed by using 6 mL of aqueous solution containing PVP (30 mg) in place of I-Cage–Cl.

Catalytic activity characterization

Procedure for the hydrolysis of AB by Pt@I-Cage–Cl catalyst. The reaction apparatus for measuring the hydrogen evolution from the hydrolysis of AB is as follows. In general, the as-synthesized Pt@I-Cage–Cl catalyst was placed in a two-necked round-bottomed flask (30 mL), which was placed in a water bath under ambient atmosphere. A gas burette filled with water was connected to the reaction flask to measure the volume of hydrogen. The reaction started when AB (15 mg) in 0.5 mL water was added into the flask. The volume of the evolved hydrogen gas was monitored by recording the displacement of water in the gas burette. The reaction was completed when there was no

more gas generation. The hydrolysis of AB can be expressed as follows:

$$NH_3BH_3 + 2H_2O \rightarrow NH_4BO_2 + 3H_2 \qquad (1)$$

Procedures for the hydrolysis of AB by Pt/RCC3, Pt-SP-Free, Pt/CTAB and Pt/PVP catalysts. The procedures for the hydrolysis of AB were identical to that of Pt/I-Cage–Cl catalyst except different catalysts were used.

Results and discussion

The targeted ionic cage molecule (denoted as I-Cage–Cl, Cl as counterion), $[(H_{12}RCC3)^{12+}12Cl^-]$, was synthesized according to a recent report by HCl-acidifying a neutral amine cage RCC3 (Scheme S1†).[12a,b] Each I-Cage–Cl carries 12 cations and was characterized by ^{1}H and ^{13}C NMR spectra and mass spectrometry (Fig. S1–S3†). The hydrophilic ammonium chloride ion pair makes I-Cage–Cl readily water-soluble, while its neutral precursor RCC3 is insoluble. The cryo-EM image (Fig. S4†) of I-Cage–Cl reveals well-dispersed dark dots of 3 ± 0.4 nm in size, slightly larger than its precursor RCC3 of ~2 nm in size (cryo-EM image in Fig. S5,† which is in agreement with size estimation from its octahedron architecture[12b]). The size expansion from RCC3 to I-Cage–Cl is expected as the ionized –NH– units electrostatically stretch the cage and the newly introduced Cl$^-$ also expand its overall hydrodynamic size.

Due to a high cation density on the cage, the coulombic attraction and the confinement effect facilitate encapsulation of metal anions into I-Cage–Cl as host, as reported recently for a host of metals on different supports.[13] Principally, the reduction of encapsulated metal anions and the subsequent nucleation within the cage host is expected and downsizes MCs to match the cage cavity. Experimentally this process runs as follows: a pale yellow solution of I-Cage–Cl (15 mg) in 9 mL of water was prepared. It became light brown upon addition of HAuCl$_4$ (Au content: 0.5 mg). The interaction between the cationic cage and $[AuCl_4]^-$ was monitored by zeta potential analysis, in which an initial value of +38.9 mV of I-Cage–Cl drops to +28.6 mV upon addition of HAuCl$_4$ due to specific adsorption/complexation of $[AuCl_4]^-$ by I-Cage–Cl. Addition of NaBH$_4$ at r.t. produced a pale brown, stable MC solution.

DLS study (Fig. S6†) and cryo-EM analysis (Fig. 1a) determine the as-synthesized Au@I-Cage–Cl be to 3.0 nm and 3.1 ± 0.4 nm, respectively, in good consistence with the size value of native I-Cage–Cl. The size of Au clusters was determined by high-angle annular dark-field scanning transmission electron microscopy (HAADF-STEM) to be 0.65 ± 0.2 nm (Fig. 1b and S7a†), which matches well with the pore size of RCC3 cage (~0.72 nm), indicative of possibility of cage encapsulation. Such small cluster size agrees well with the absence of a Plasmon peak in the UV-Vis spectrum (Fig. 2b). XPS data identify peaks of binding energy at 88.4 and 84.4 eV, corresponding to $4f_{5/2}$ and $4f_{7/2}$ of metallic Au existed in the cage (Fig. S8†).

The NMR technique is applied to better analyze Au@I-Cage–Cl and specifically, the spatial relationship between the cage host and the Au cluster guest. The ^{13}C NMR spectra of Au@I-Cage–Cl (Fig. S2b†) and I-Cage–Cl (Fig. S2a†) show little-to-no

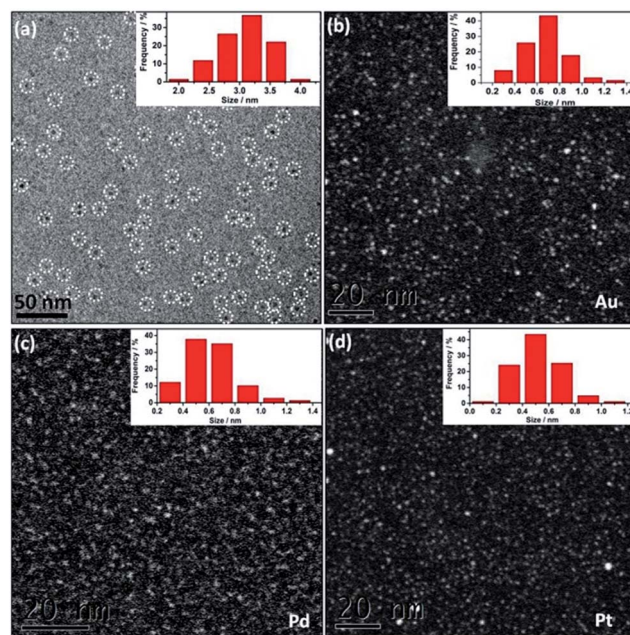Fig. 1 (a) Cryo-EM image of Au@I-Cage–Cl on a Lacey carbon grid and the size distribution histogram. Some Au@I-Cage–Cl are highlighted by white dotted circles. (b–d) HAADF-STEM images and the size distribution histograms of Au, Pd and Pt clusters, respectively.

variation in peak positions, suggesting that I-Cage–Cl is in an approximate configuration before and after encapsulation of MCs. Interestingly, in comparison to I-Cage–Cl (Fig. S1a†), broadening of all peak widths in the ^{1}H NMR spectrum of Au@I-Cage–Cl (Fig. S1b†) is observed, indicative of a local restricted motion and structural heterogeneity stemming from encapsulation of Au clusters.[14,12c] A similar observation was reported in Au NPs@Cage (average Au NP size: 1.9 nm),[14a] in which the cage shell tightly wrapped around the AuNP, and experienced restricted mobility and fast spin relaxation. Further evidence was given by 2D diffusion ordered spectroscopy ^{1}H nuclear
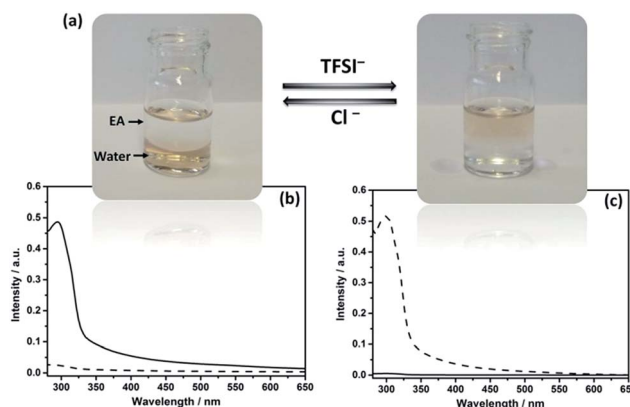

Fig. 2 (a) Photographs showing reversible transfer of Au–I-Cage–X (X = Cl$^-$ or TFSI$^-$) between aqueous and EA phases upon anion exchange. (b and c) UV-Vis spectra of Au clusters transferred between aqueous and EA phases (solid curve for aqueous phase, dotted curve for EA phase) as shown in (a).

magnetic resonance (2D DOSY ^{1}H NMR) (Fig. S9 and S10†) that shows similar diffusion coefficients for Au@I-Cage–Cl (2.16×10^{-6} cm^2 s^{-1}) and I-Cage–Cl (2.06×10^{-6} cm^2 s^{-1}), confirming the similar size and shape of native I-Cage–Cl and Au@I-Cage–Cl. Such observation proves that Au clusters rest inside the cage cavity instead of intercage interactions or aggregation on the cage surface.[14a,12c] In addition, the size of Au@I-Cage–Cl determined by cryo-EM data in Fig. 1a and DLS (consistent with single native I-Cage–Cl cage) excludes the possibility of Au clusters stabilized by multiple cages.

Cage-confinement brings Au clusters high stability. For example, storage in a temperature range from 77 to 363 K and in a pH range from 3 to 10 did not change the cluster size, as confirmed by UV-Vis spectra (Fig. S11†) and HAADF-STEM analysis (Fig. S12–S15†). Rationally the electrostatic repulsion separates molecular cages and each octahedron cage sterically contains individual MCs well inside.[15] In a control experiment without I-Cage–Cl, only aggregated Au NPs were observed (Fig. S16†). Using neutral cage RCC3 as support produced Au NPs of a larger size of 4 ± 0.8 nm with a broader size distribution and poor solubility in water (Fig. S17†). Moreover, a monovalent ionic liquid (IL) 4-cyanomethyl-1-vinyl-imidazolium bromide, when used in the same experiment, resulted in Au NPs of 6 ± 0.9 nm in size (Fig. S18†). Therefore, the cage-ion synergy plays a pivotal role in size control. It is worth noting that our method can produce other noble MCs, *i.e.* 0.6 ± 0.2 nm for Pd (Fig. 1c and S7b†) and 0.5 ± 0.2 nm for Pt clusters (Fig. 1d and S7c†).

In IL chemistry, hydrophilicity/hydrophobicity of ILs is switchable by ion metathesis.[16] Here, as a proof of concept, Au@I-Cage–Cl was modified into hydrophobic Au@I-Cage–TFSI bearing bis(trifluoromethane sulfonyl)imide (TFSI) anion by anion exchange[17] with LiTFSI (Scheme 1b). Experimentally, hydrophobic ethyl acetate (EA) was first added to a pale brown Au@I-Cage–Cl aqueous solution to form a clear supernatant. Addition of LiTFSI formed a colorless aqueous phase and a pale brown EA phase (Fig. 2a). Residue Au@I-Cage–Cl in the aqueous phase produced a negligible absorbance peak at $\lambda = 300$ nm (assigned to I-Cage) in its UV-Vis spectrum, while the EA phase shows a characteristic absorbance spectrum of I-Cage, indicative of a quantitative phase transfer (Fig. 2c). A similar behavior was observed when Au clusters were reversed to aqueous phase by adding KCl (Fig. 2b). ICP-OES measurement shows <5 ppm loss of Au (Fig. S19†) during this cycle, indicative of its reversible nature. Such process can be repeated two times without significantly altering the intensity and position of cage peak in UV-Vis spectrum (Fig. S20†). Additionally, DLS (Fig. S21†), cryo-EM (Fig. S22†) and HAADF-STEM analyses did not show any size increase (Fig. S23a–c†) for Au cluster, as also for Pd and Pt (Fig. S23d–i, S24 and S25†). Worth to mention is that such feature is valuable, as it combines the physical confinement effect with ion exchange capability, which fails in conventional organic ligands.

Being physically confined and phase transferable is useful, as it allows the same MC catalyst for operations in different liquids while strictly keeping their size. Tested in a H$_2$ release reaction by hydrolysis of AB compound,[18] Pt@I-Cage–Cl at a Pt
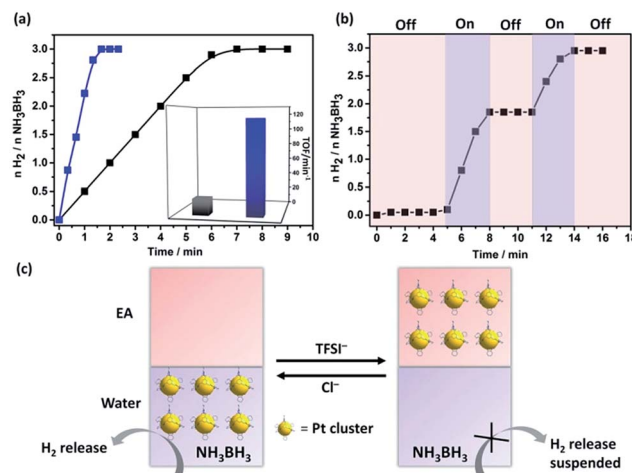

Fig. 3 (a) Time course plots of H$_2$ generation for the hydrolysis of ammonia borane (AB) over the Pt@I-Cage–Cl (blue line) and unsupported Pt catalysts, Pt-SP-Free (dark line) at 300 K (Pt/AB = 0.02). Inset: the corresponding TOF values. (b) Control of H$_2$ release in the AB hydrolysis in water–EA mixture (pink and violet regions for "off" and "on" state, respectively). (c) Diagram of controlled H$_2$ release process.

loading content of 0.01 mmol (Pt/AB = 0.02) completed the reaction (H$_2$/AB = 3.0) within 1.3 min at 300 K (Fig. 3 and S26†). The turnover frequency (TOF) is 115 min^{-1}, which is much higher than conventional surfactant-protected catalysts (Fig. S27–S30†), *e.g.* Pt/CTAB (2.7 ± 0.3 nm, TOF: 5 min^{-1}), Pt/PVP (4 ± 0.4 nm, TOF: 13 min^{-1}), and RCC3-supported Pt NPs (Pt/RCC3, 3 ± 0.6 nm, TOF: 30 min^{-1}) (Fig. S31 and 32†), and comparable to the reported highly active monometallic Pt cluster/nanoparticle catalysts.[19] Not surprising, a low TOF value of 20 min^{-1} was found for cage-free Pt nanoparticles (Pt-SP-Free) (Fig. 3 and S33†). Although I-Cage–Cl itself is catalytically inactive to AB (tested in Fig. S34†), the discrete open structure can promote catalytic reactions by downsizing Pt clusters and maximizing metal–reactant contact in solution.

The phase-transfer process is useful to recover and recycle catalyst. Typically, after completion of a reaction, Pt clusters were transferred to the EA phase by LiTFSI. The impure aqueous phase was replaced by clean water, before Pt clusters moved back by adding KCl for the next run (Fig. S35†). Uniquely, the anion exchange could regulate the H$_2$ production. As shown in Fig. 3b and c, H$_2$ generation was stopped upon addition of LiTFSI to evacuate Pt clusters from water; the reaction re-started by adding KCl to transfer Pt clusters back. This "on"/"off" cycle can be repeated till AB is consumed. Our system provides a new insight toward kinetic control for on-demand H$_2$ release in practical use.

Conclusions

In conclusion, a method to prepare sub-nano-sized noble MCs hosted by an ionic organic cage was reported. The reversible anion exchange process enables confined MCs to be shuttled selectively between an aqueous and an organic phase, which allows for efficient separation and recycling of MC catalysts

from products or reaction mixtures. This method will equip researchers with a new tool to engineer MCs without compromising their catalytic activity, thus improving and augmenting applications in different research areas.

Conflicts of interest

There are no conflicts to declare.

Acknowledgements

Notes and references

1 (a) J. P. Wilcoxon and B. L. Abrams, *Chem. Soc. Rev.*, 2006, **35**, 1162; (b) Y. Lu and W. Chen, *Chem. Soc. Rev.*, 2012, **41**, 3594; (c) F. Schüth, *Angew. Chem., Int. Ed.*, 2014, **53**, 8599; (d) G. Li and R. Jin, *Acc. Chem. Res.*, 2013, **46**, 1749; (e) J. Zhang, Y. Yuan, G. Liang, M. N. Arshad, H. A. Albar, T. R. Sobahi and S. H. Yu, *Chem. Commun.*, 2015, **51**, 10539; (f) X. Tuaev, J. P. Paraknowitsch, R. Illgen, A. Thomas and P. Strassera, *Phys. Chem. Chem. Phys.*, 2012, **14**, 6444; (g) J. Lin, Q. Zhang, L. Wang, X. Liu, W. Yan, T. Wu, X. Bu and P. Feng, *J. Am. Chem. Soc.*, 2014, **136**, 4769; (h) J. Yang, R. Fainblat, S. G. Kwon, F. Muckel, J. H. Yu, H. Terlinden, B. H. Kim, D. Iavarone, M. K. Choi, I. Y. Kim, I. Park, H. K. Hong, J. Lee, J. S. Son, Z. Lee, K. Kang, S. J. Hwang, G. Bacher and T. Hyeon, *J. Am. Chem. Soc.*, 2015, **137**, 12776; (i) R. R. Nasaruddin, T. Chen, N. Yan and J. Xie, *Coord. Chem. Rev.*, 2018, **368**, 60; (j) F. R. Fortea-Pérez, M. Mon, J. Ferrando-Soria, M. Boronat, A. Leyva-Pérez, A. Corma, J. M. Herrera, D. Osadchii, J. Gascon, D. Armentano and E. Pardo, *Nat. Mater.*, 2014, **16**, 760.

2 Q. Yao, X. Yuan, Y. Yu, J. Xie and J. Y. Lee, *J. Am. Chem. Soc.*, 2015, **137**, 2128.

3 (a) A. Dong, X. Ye, J. Chen, Y. Kang, T. Gordon, J. M. Kikkawa and C. B. Murray, *J. Am. Chem. Soc.*, 2011, **133**, 998; (b) J. Yang, E. H. Sargent, S. O. Kelley and J. Y. Ying, *Nat. Mater.*, 2009, **8**, 683; (c) L. Peng, M. You, C. Wu, D. Han, I. Ocsoy, T. Chen, Z. Chen and W. Tan, *ACS Nano*, 2014, **8**, 2555.

4 J. C. Vickery, M. M. Olmstead, E. Y. Fung and A. L. Balch, *Angew. Chem., Int. Ed.*, 1997, **36**, 1179; G. G. Shan, D. X. Zhu, H. B. Li, P. Li, Z. M. Su and Y. Liao, *Dalton Trans.*, 2011, **40**, 2947.

5 (a) A. Stocco, M. Chanana, G. Su, P. Cernoch, B. P. Binks and D. Wang, *Angew. Chem., Int. Ed.*, 2012, **51**, 9647; (b) B. Qin, Z. Zhao, R. Song, S. Shan and Z. Tang, *Angew. Chem., Int. Ed.*, 2008, **47**, 9875; (c) S. Ye, A. V. Zhukhovitskiy,

C. V. Deraedt, F. D. Toste and G. A. Somorjai, *Acc. Chem. Res.*, 2017, **50**, 1894; (d) J. Yang, J. Y. Lee and J. Y. Ying, *Chem. Soc. Rev.*, 2011, **40**, 1672; (e) T. V. Richter, C. Bîhler and S. Ludwigs, *J. Am. Chem. Soc.*, 2012, **134**, 43.

6 (a) N. Xia, J. Yang and Z. Wu, *Nanoscale*, 2015, **7**, 10013; (b) X. Yuan, Z. Luo, Q. Zhang, X. Zhang, Y. Zheng, J. Y. Lee and J. Xie, *ACS Nano*, 2011, **5**, 8800; (c) J. X. Dong, Z. F. Gao, Y. Zhang, B. L. Li, W. Zhang, J. L. Lei, N. B. Li and H. Q. Luo, *NPG Asia Mater.*, 2016, **8**, 335; (d) S. Knoppe, O. A. Wong, S. Malola, H. Hakkinen, T. Bürgi, T. Verbiest and C. J. Ackerson, *J. Am. Chem. Soc.*, 2014, **136**, 4129.

7 (a) T. Pellegrino, L. Manna, S. Kudera, T. Liedl, D. Koktysh, A. L. Rogach, S. Keller, J. Rädler, G. Natile, W. J. Parak, N. D. Burrows, E. Kesselman and K. Sabyrov, *Nano Lett.*, 2004, **4**, 703; (b) A. Stemig, Y. Talmon and R. L. Penn, *CrystEngComm*, 2014, **16**, 1472.

8 J. K. Sun, Z. Kochovski, W. Y. Zhang, H. Kirmse, Y. Lu, M. Antonietti and J. Yuan, *J. Am. Chem. Soc.*, 2017, **139**, 8971.

9 (a) T. Tozawa, J. T. A. Jones, S. I. Swamy, S. Jiang, D. J. Adams, S. Shakespeare, R. Clowes, D. Bradshaw, T. Hasell, S. Y. Chong, C. Tang, S. Thompson, J. Parker, A. Trewin, J. Bacsa, A. M. Z. Slawin, A. Steiner and A. I. Cooper, *Nat. Mater.*, 2009, **8**, 973; (b) G. Zhang, O. Presly, F. White, I. M. Oppel and M. Mastalerz, *Angew. Chem., Int. Ed.*, 2014, **53**, 1516; (c) F. Beuerle and B. Gole, *Angew. Chem., Int. Ed.*, 2018, **57**, 4850; (d) E. J. Dale, N. A. Vermeulen, A. A. Thomas, J. C. Barnes, M. Juríček, A. K. Blackburn, N. L. Strutt, A. A. Sarjeant, C. L. Stern, S. E. Denmark and J. F. Stoddart, *J. Am. Chem. Soc.*, 2014, **136**, 10669.

10 (a) J. K. Sun, W. W. Zhan, T. Akita and Q. Xu, *J. Am. Chem. Soc.*, 2015, **137**, 7063; (b) B. Mondal, K. Acharyya, P. Howlader and P. S. Mukherjee, *J. Am. Chem. Soc.*, 2016, **138**, 1709; (c) Y. Fang, J. F. Li, T. Togo, F. Y. Jin, Z. F. Xiao, L. J. Liu, H. Drake, X. Z. Lian and H. C. Zhou, *Chem*, 2018, **4**, 555.

11 (a) M. Mokhadinyana, S. L. Desset, D. Bradley, G. Williams and D. J. Cole-Hamilton, *Angew. Chem., Int. Ed.*, 2012, **51**, 1648; (b) Y. Brunsch and A. Behr, *Angew. Chem., Int. Ed.*, 2013, **51**, 1586; (c) D. E. Bergbreiter, *ACS Macro Lett.*, 2014, **3**, 260.

12 (a) M. Liu, M. A. Little, K. E. Jelfs, J. T. A. Jones, M. Schmidtmann, S. Y. Chong, T. Hasell and A. I. Cooper, *J. Am. Chem. Soc.*, 2014, **136**, 7583; (b) M. Liu, L. Chen, S. Lewis, S. Y. Chong, M. A. Little, T. Hasell, I. M. Aldous, C. M. Brown, M. W. Smith, C. A. Morrison, L. J. Hardwick and A. I. Cooper, *Nat. Commun.*, 2016, **7**, 12750; (c) X. Yang, J. K. Sun, M. Kitta, H. Pang and Q. Xu, *Nat. Catal.*, 2018, **1**, 214.

13 (a) A. Wong, Q. Liu, S. Griffin, A. Nicholls and J. R. Regalbuto, *Science*, 2017, **358**, 1427; (b) G. Yun, Z. Hassan, J. Lee, J. Kim, N. S. Lee, N. H. Kim, K. Baek, I. Hwang, C. G. Park and K. Kim, *Angew. Chem., Int. Ed.*, 2014, **53**, 6414.
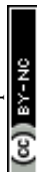
14 (*a*) R. McCaffrey, H. Long, Y. Jin, A. Sanders, W. Park and W. Zhang, *J. Am. Chem. Soc.*, 2014, **136**, 1782; (*b*) T. Inomata and K. Konishi, *Chem. Commun.*, 2003, 1282; (*c*) A. C. Templeton, W. P. Wuelfing and R. W. Murray, *Acc. Chem. Res.*, 2000, **33**, 27.

15 (*a*) P. Zhang, Z. A. Qiao, X. Jiang, G. M. Veith and S. Dai, *Nano Lett.*, 2015, **15**, 823; (*b*) J. K. Sun, M. Antonietti and J. Yuan, *Chem. Soc. Rev.*, 2016, **45**, 6627.

16 (*a*) G. T. Wei, Z. Yang, C. Y. Lee, H. Y. Yang and C. R. Chris Wang, *J. Am. Chem. Soc.*, 2004, **126**, 5036; (*b*) T. Welton, *Chem. Rev.*, 1999, **99**, 2071.

17 (*a*) A. B. Grommet and J. R. Nitschke, *J. Am. Chem. Soc.*, 2017, **139**, 2176; (*b*) S. Löffler, J. Lübben, L. Krause, D. Stalke, B. Dittrich and G. H. Clever, *J. Am. Chem. Soc.*, 2015, **137**, 1060; (*c*) D. Luo, X. P. Zhou and D. Li, *Angew. Chem., Int. Ed.*, 2015, **54**, 6190; (*d*) C. J. Bruns, D. Fujita, M. Hoshino, S. Sato, J. F. Stoddart and M. Fujita, *J. Am. Chem. Soc.*, 2014, **136**, 12027.

18 (*a*) A. Gutowska, L. Li, Y. Shin, C. M. Wang, X. S. Li, J. C. Linehan, R. S. Smith, B. D. Kay, B. Schmid, W. Shaw, M. Gutowski and T. Autrey, *Angew. Chem., Int. Ed.*, 2005, **44**, 3578; (*b*) R. J. Keaton, J. M. Blacquiere and R. T. Baker, *J. Am. Chem. Soc.*, 2007, **129**, 1844; (*c*) M. Yadav and Q. Xu, *Energy Environ. Sci.*, 2012, **5**, 9698.

19 W. Zhan, Q. L. Zhu and Q. Xu, *ACS Catal.*, 2016, **6**, 6892.